

Maximizing network coverage in a multichannel short-range underwater acoustic sensor network

Hossein Ghannadrezaii*, Jean-François Bousquet

Electrical and Computer Engineering, Dalhousie University, Halifax, Canada



ARTICLE INFO

Article history:

Received 22 February 2018

Revised 14 May 2019

Accepted 15 May 2019

Available online 20 May 2019

Keywords:

Underwater acoustic sensors network

Distributed channel allocation

Network coverage

Fair channel allocation

Interference graph

ABSTRACT

In this paper, a Media Access Control (MAC) protocol is investigated for multichannel underwater acoustic sensor networks and a distributed channel allocation scheme is proposed for acoustic nodes equipped with a multichannel bi-directional transceiver. To ensure that a minimum of one channel is allocated for each transmitter-receiver pair, a novel distributed channel allocation scheme, the High Coverage High Fairness (HCHF) algorithm, is proposed. The algorithm requires the exchange of channel sensing information among neighbor nodes at the beginning of each transmission time slot. To compare HCHF and existing schemes, various performance metrics are assessed including spectrum utilization, coverage, fairness, and control packet overhead. Simulation results indicate that the HCHF scheme can improve the coverage and fairness in comparison to other schemes without sacrificing much on the spectrum utilization. The performance improvement of HCHF is constrained by a higher control message overhead, since local packet exchange between neighbor nodes is required to share spectrum sensing information.

© 2019 Elsevier B.V. All rights reserved.

1. Introduction

The deployment of underwater networks is attracting significant interest to monitor subsea infrastructure, and submarine activity. Enabling underwater acoustic sensor networks (UWASNs) is key for ocean monitoring and data collection. For example, commercial and scientific UWASN applications target oil and gas and aquaculture industries and include instrument monitoring, pollution control, climate recording, offshore exploration and pipeline surveillance. Moreover, the Internet of Underwater Things (IoUT) extends the Internet of Things (IoT) to subsea applications, and interconnects a large number of sensors of various types to collect data in a distributed fashion for various applications [1]. However, UWASN impose challenges to the IoUT due to the band-limited underwater acoustic channels.

The primary design goal of the proposed underwater wireless network is to exchange sensor information using acoustic nodes (ANs). A multi-hop peer-to-peer network is formed by establishing communication links only between neighboring nodes. Messages are transferred from source to destination by hopping packets from node to node [2]. For this purpose, it is important to define a distributed channel allocation scheme. An important challenge is that the communication resources are limited: acoustic propaga-

tion presents a limited bandwidth and it depends on the geometry of the deployment which varies as a function of time and location [3]. Also, the channel is time variant and fluctuates rapidly due to low propagation speed. To optimize the network spectral usage, the nodes are aware of their surrounding medium and acoustic spectrum to adjust the transceiver parameters, e.g. the transmit power and the selected channel frequency band. Consequently, each node in the UWASN must first sense and determine the available slots in the frequency spectrum and cooperate with other nodes to grant a channel.

In this paper, a novel distributed scheme, the High Coverage and High Fairness (HCHF) algorithm, is proposed which employs a graph coloring technique to deal with interference [4]. HCHF improves the network coverage by ensuring that each transmitter-receiver pair can acquire at least one channel without sacrificing the entire network spectrum utilization efficiency. This ensures connectivity throughout the network and thus enables packet forwarding and routing between multiple nodes. To optimize the use of the sparse spectral resources, a channel sharing strategy among users will be developed to optimize the network connectivity and throughput.

In this work, the network path connectivity is guaranteed by ensuring that all transmitter-receiver pairs obtain access to at least one channel. Coverage, defined as the number of connected cognitive acoustic pairs, as well as fairness, defined as the number of pairs which obtain at least one channel, are two key figures of merit used to assess the performance.

* Corresponding author.

E-mail addresses: h.ghannadrezaii@dal.ca (H. Ghannadrezaii), JBousquet@Dal.ca (J.-F. Bousquet).

The rest of this paper is organized as follows: in Section 2, comparable algorithms that serve for spectrum allocation in underwater sensor networks are reviewed, in Section 3, the network model is introduced, in Section 4 the channel allocation algorithm in the UWASN is compared to state-of-the-art, in Section 5, simulation results are analyzed, and finally, in Section 6, conclusions are presented.

2. Related work

The standardization of the MAC protocol to enable UWASNs remains a very important subject of research. Indeed, the narrow bandwidth on the order of a few kHz is a limiting factor. Also, the long propagation delay increases the probability of collision. Some recent efforts have been made to enable multichannel spectrum management techniques for distributed networks, but, due to the features of underwater acoustic communications, existing schemes may not work effectively. Relevant works in this field is summarized in this section.

In [5], the authors describe a MAC protocol, called CUMAC to handle the hidden terminal problem, i.e. when unreported nodes cause collisions in underwater multichannel networks. This problem is particularly important when there is a long distance between the nodes. Using CUMAC, when a node has packets to send, it initiates a channel negotiation process on the control channel. During this process, the receiving node cooperates with its neighboring nodes for channel selection and collision detection. In [5], although the hidden terminal problem and collision avoidance are addressed, the channel assignment mechanism is not considered because the spectrum demand is assumed low.

In [6], the authors propose a channel allocation scheme which exploits user location knowledge in order to maximize the minimum channel capacity achieved by each individual user. Fairness and efficient use of the available spectrum resources are the primary criteria to allocate channels. Assuming a network with N users, for a given channel allocation of a , the authors define the capacity vector $\mathbf{c}_a = [c_{a,1}, c_{a,2}, \dots, c_{a,N}]$. In the vector \mathbf{c}_a , the entry at index i indicates the potential channel capacity $c_{a,i}$ for user i . A feasible channel allocation b is said to have a Max-Min fair allocation if, for any other feasible allocation a , $c_{a,i} \leq c_{b,i}$ holds for all i . One of the key points of the algorithm is how to determine whether a feasible solution exists. When there are N available channels, $N^4 \times \sqrt{N}$ steps are performed by this Max-Min capacity channel allocation algorithm. As such, the computational complexity of this algorithm is excessive. Also, the interference between neighbors on the same available channels of interest and the hidden terminal problem are issues which are not addressed. Additional shortcomings appear when two or more nodes have the same feasible channel to allocate with the same capacity. This can occur when the network is dense, and the nodes are relatively close to each other.

In [7], the authors propose a cluster-based random-access method by grouping nodes located close to a fusion node. Effectively, this grouping decreases the probability of message collisions due to long delay propagation time between nodes. To reduce the collision probability, each node selects its group, which is predetermined by its distance from the fusion center based on the received signal strength (RSS). The start of the transmission time for all nodes is synchronized with that of the furthest node in the group. Nodes choose the data frequency band based on the RSS. In [7], the number of ANs are relatively small, they have different distances from the fusion center and as such they experience different RSS. Effectively, the channel access scheme is contention free due to high availability of the spectrum. In contrast, for the proposed dense network, there is a high spectrum demand. Also, nodes that are within the same range to the fusion node will experience very similar RSS, and collision is highly probable.

In [8], the authors propose a receiver-initiated spectrum management technique that seeks to improve the performance of UWASNs by utilizing a traffic predictor on each node to forecast the traffic load on surrounding nodes. For this purpose, each node must have knowledge of the propagation delay to its neighbors. The common control channel (CCC) is physically separated from the in-band data channel. The use of a CCC within a different band increases the complexity of the front-end design. Nonetheless, by using the CCC, and by collecting local sensing results from its neighbors, the receiver obtains global spectrum usage information. Using this information, the receiver assigns vacant channels and an optimal transmission power for its surrounding transmission nodes based on the spectrum sensing output and the quality of the acoustic links. Note that the algorithm does not address the situation when there is high spectrum demand. Also, because a minimum traffic is required to allocate the channels, an unfair scenario occurs for nodes which have lower traffic, since they have to wait longer.

In [9], a spectrum allocation method, the Link Degree and Round Based Algorithm (LDRA), is proposed. For LDRA, the link degree is used as a criterion for allocation. Specifically, a node link degree on a given channel is defined as the number of neighbors interfering with the node on that channel. Thus, a node with less interfering neighbors has a lower link degree. The LDRA algorithm allocates the available channels to the nodes with the smallest link degree until no channel can be chosen. If there are two or more nodes with the same link degree, the channel is allocated randomly between them. If there are still available channels, the LDRA algorithm initiates the next distribution round; otherwise, the algorithm ends. Although this algorithm considers a maximum spectrum utilization it does prevent nodes subject to high interference from having a channel.

Finally, in [10], the authors suggest a graph-coloring model based on a frequency band allocation algorithm which combines the greedy allocation approach and interference constraints. They use a graph model for the cognitive network in which the vertices represent the neighbor nodes and the edges represent interference among them. The graph then identifies a set of available channels associated to each vertex. The proposed Max-Min algorithm allocates the frequency band with the largest channel gain from the list of available frequency bands for each node. The algorithm iteratively allocates the user with the minimum transmission rate to the frequency band with the largest channel gain in the available list, until all the frequency bands are allocated. While this algorithm uses a greedy allocation scheme to maximize the resource allocation, it does not guarantee allocating a minimum of one channel to each node.

Although there is a significant amount of work that has been performed in recent years towards the deployment of UWASNs, there is still a gap that needs to be filled to address the channel allocation problems in UWASN. The algorithm proposed here is intended to model and solve channel allocation problem in dense UWASN with high spectrum usage demand while dealing with interference. The network is intended to support the IoUT and it can be expected that up to a few hundred sensor nodes with different purposes will be deployed in a target area spanning 10 km².

Also, practical issues such as collision avoidance and the hidden terminal problem will be taken into consideration during the design of the HCHF protocol, and will be presented in the next section.

3. Model of control and data channels

Considering a reference architecture of the UWASN [11] as depicted in Fig. 1, it consists of ANs as well as cluster heads that also act as underwater gateways (UWGs). The UWGs are equipped with

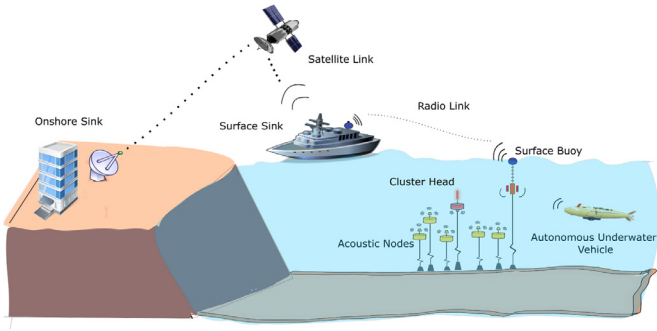


Fig. 1. Representation of a reference UWASN architecture [11].

an additional long-range vertical transceiver to relay the data of the ANs (assumed to be deployed in the middle of the water column) to the surface buoys. Cluster heads respect a cellular architecture and cover a delimited area below the water surface. Surface buoys are also equipped with a long-range radio or satellite transceiver to communicate with an onshore sink or a surface sink.

While centralized channel access management and synchronization by a cluster head has low complexity and energy dissipation, many challenges arise with such an architecture. Specifically, in a centralized topology the covered area is limited and all the traffic goes through the cluster head node. As such, when there is excessive traffic, when the channel quality is poor or when the cluster head node is unavailable, the sink cluster head sub-net becomes unresponsive and all the nodes within the cluster head's coverage lose their connection. In this work we consider a self-configured distributed channel assignment scheme among ANs which can be extended to a multihop relaying among ANs [12].

In this section, the proposed network channels, communication system structure and a required negotiation phase to exchange control packets, between neighbor nodes will be defined. Then, the role of the graph model to obtain the matrix of interference among neighbor nodes will be described. The graph model serve in the channel allocation algorithm proposed in Section 4.

3.1. Acoustic channels characteristics

To solve the channel allocation problem for a dense short-range UWASN with K ANs where each node is identified by an ID from $[1, 2, \dots, K]$, first a network channels model is introduced. It is assumed that the limited available spectrum is divided into M orthogonal equal bandwidth channels, presented as $[1, 2, \dots, M]$ and $M \ll K$. Moreover, one common control channel (CCC) is dedicated for the exchange of the network management controlling messages. The CCC should be the most reliable local channel for exchanging MAC packets among the neighbor ANs. Note that single-hop network is considered in this work.

It is assumed that each AN can send and receive on all channels. Every node is aware of the local CCC and listens to this channel when it has no data to send or receive. To decrease the hardware complexity each node is equipped with a single wideband transceiver front-end that can dynamically switch between the CCC and available data channels. Further, each node is equipped with an inexpensive out-of-band tone device which can broadcast and receive busy tone signals. As explained in [13,14] this allows each node to simultaneously broadcast and receive busy tone signals to solve the multichannel hidden terminal problem for nodes with single transceiver described in [15]. It is expected that high-quality filters shall serve to mitigate self-interference. The use of the busy tone to handle the hidden terminal problem will be explained in Section 4.

For the proposed network under study, there are several TX–RX pairs in the network that intend to utilize the available channels. The location of the nodes and the channel condition may vary with time and the goal is to optimally assign the channels to the TX–RX pairs in terms of spectrum utilization, coverage, and fairness at any given time.

To model the channel allocation algorithm, every node x that is within the transmission range R_T of the node y is considered a neighbor node of y . Therefore, two nodes do not interfere with each other if their distance is larger than a range R_T , where R_T is considered to represent the radius of a circular transmission range from each node [16].

For a reliable network modeling, it is important to evaluate the channel transmission loss. As explained in [17], the channel amplitude is impacted by a large scale transmission loss (that can be assessed using ray tracing simulators for example) added to a small-scale variation because of the non-coherence addition of multipath arrivals. Generally, the small-scale variation of the amplitude is modelled as a Rician distribution, or in the extreme case as a Rayleigh distribution [18,19]. Assuming a Rayleigh fading channel, a rule of thumb is to add 30 dB to the transmission loss to account for extreme small scale variation.

It is also important to consider the coherence time for underwater acoustic channels [20] which is defined as

$$\tau_c = \sqrt{\frac{9}{16\pi f_d^2}} \approx \frac{0.423}{f_d} \approx \frac{0.423}{a f_c}. \quad (1)$$

where f_d is the Doppler spread, f_c is the carrier frequency, and a is the Doppler scaling factor. As explained in [21], a stationary underwater acoustic system may experience unintentional motion at 0.5 m/s (1 kn), which would account for $a = 3 \times 10^{-4}$. In contrast an autonomous underwater vehicle (AUV) moving at several meters per second, Doppler factor a will be on the order of 10^{-3} . In fact, it has been reported in [22,23] that the coherence time is on the order of 100 ms in fixed conditions, while the channel between mobile vehicles can experience a channel coherence time on the order of a few milliseconds. It is assumed that the sound speed c in the water column between the transmitters and receivers has a constant velocity of $c = 1500$ m/s. The propagation delay, $T_p = R/c$, for the expected transmission range, $R = 500$ m between the nodes will be about 334 ms.

Since underwater transmission is slow, the packet duration is often longer than the channel coherence time. For this purpose, in this work it is assumed that the physical layer is resilient to Doppler fading within the transmission of packets. Since frequency-hopping binary frequency shift keying (FH–BFSK) is used in this work, the binary information is represented using different frequency tones. As will be demonstrated, since the coherence time is greater than a few milliseconds, the channel is expected to stay relatively constant during the transmission of the individual tones. Transmission of acoustic signals will be described in the next section.

3.2. FH–BFSK underwater acoustic communication system

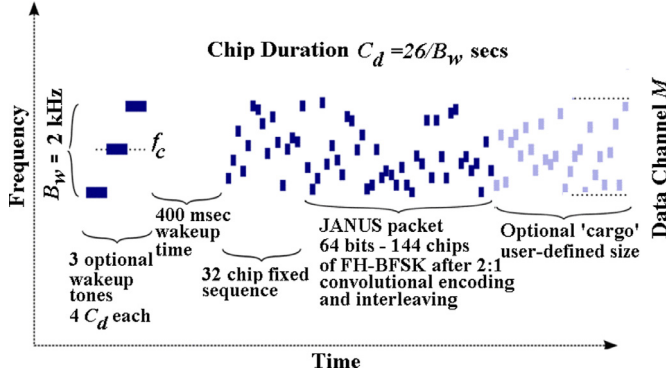
In this work, an UWASN is considered in which 10 distinct 2-kHz channels are defined over a total frequency range between 10.5 kHz and 30.5 kHz. For mobile AUVs where $a = 10^{-3}$, the maximum Doppler shift, which is defined as $f_d = a \times f_c$, is less than ± 30.5 Hz [24] at $f_c = 29.5$ kHz. To mitigate the maximum Doppler shift a guard band of 77 Hz is considered between the channels.

The duration of each individual tone is called chip duration C_d . Using (1), for mobile AUVs with a maximum speed of 7 kn, tone signals with a maximum chip duration of $C_d \approx 14$ ms can be sent.

To break the interoperability barrier and enable collaborative underwater communications, the JANUS baseline packet structure,

Protocol Version	Mobility Flag	Scheduling Bit	Tx/Rx	Forward Capability	User Class	Application Type	Repetition	ADB		CRC
								Reserved or Repeat interval	Node Information	
4	1	1	1	1	8	6	1	7	26	8

Fig. 2. JANUS Packet Bits 1 to 64.

Fig. 3. The JANUS signal for channel M in a time-frequency plot [26].

which is a NATO standard for digital underwater communications, is used in this work. Using a standardized protocol enables communication and packet forwarding among heterogeneous nodes [25]. As defined in the standard [26], the packet contains 64 bits, consisting of a 34-bit application data block (ADB) that is determined by the acoustic node. The packet is assembled according to the bit allocations shown in Fig. 2.

A JANUS baseline packet can also be complemented by a cargo section of arbitrary length. The system also employs a 1/2 rate convolutional encoder [27] that is applied to the 64 bits of JANUS packet and is intended to combat the channel multipath interference as well as fading. Prior to encoding, 8 zeros are added to the data to flush the encoder, which will be discarded at the receiver. The total number of symbols output by the encoder then becomes $2 \times (64 + 8) = 144$ [28]. A fixed preamble of 32 chips is employed for detection and synchronization. As such, altogether a JANUS packet comprises 176 chips. So, each packet duration is equal to 2288 ms.

Frequency-Hopping (FH) Binary Frequency Shift Keying (BFSK) has been selected for its robustness in the harsh UW acoustic propagation environment and for its simplicity of implementation [29]. FH-BFSK is a non-coherent physical encoding technique, which already is used in commercially-produced modems. Frequency hopping spreads the signal in frequency and time to mitigate the effects of the variable multipath. In this work, we define the hopping rate to be equal to the symbol rate, as such the chip duration is C_d and is also equal to the symbol duration. Thirteen orthogonal tones are mapped in evenly-spaced tone pairs that span the acoustic frequency bandwidth of 2-kHz of each channel, and each frequency slot width is $F_{sw} = B_w/26$. Effectively, each chip duration is $C_d = 26/B_w$, or $C_d = 13$ ms. Fig. 3 shows a time-frequency representation of a generic JANUS packet for one channel.

The proposed FH-BFSK system signal specifications for the data channels are summarized in Table 1.

3.3. Common control channel and control packets

As described in [25] Collision Avoidance (CA) via Binary Exponential Backoff (BEB) with Global Awareness (GA) consists of an in-band energy detector used to access the CCC. Transmitters

Table 1
FH BFSK signal specifications.

Parameter	Value
Number of channels, M	10
Number of sub carriers in each channel, M_{sub}	26
Sub carriers frequency slot width, F_{sw}	77 Hz
Modulation order,	2
Chip time, C_d	13 ms
Bits per Symbol, k	1 bpS
Packet duration, P_s	2288 ms

are required to sense the CCC before transmission of controlling packets for a minimum of twice the length of an encoded basic controlling packet plus the propagation delay. The control packets are smaller than the data packets and are defined by a 4-bits packet type, an 8-bit node ID and a 12-bit payload. Data corruption is detected by an 8-bit cyclic redundancy check (CRC) which is appended to the packet. These 32 bits with 8 zeros amount to $2 \times (32 + 8) + 32 = 112$ chips after encoding and assuming a fixed preamble of 32 chips. Accordingly, the CCC sensing will last for a DCF interframe spacing (DIFS) equal to $2 \times 112 \times C_d + T_p$ seconds, where T_p is packet propagation delay.

If the CCC is busy when a transmitter intends to transmit, the transmitter continues to sample windows of duration equal to $16 \times C_d$ until the CCC is deemed no longer busy. The transmitter then applies a BEB: it transmits in the next slot with probability $1/(D + 1)$, where $D = 2^C - 1$ and C is the number of potential transmissions slots the transmitter has counted in the backoff process in which there has been at least one busy window (C is initialized with $C = 1$). If the transmitter does not transmit in the first available slot, it continues to sample 16 chip windows to detect if the CCC is busy during the next slot. The node increments C by one (but only once per slot) if this is the case at any point during the slot, up to a maximum of $C = 8$. Once the TX node finds the CCC available to transmit its message, C is re-initialized to $C = 1$. If C reaches 8, the attempt to transmit that packet is abandoned.

To allocate the available channels, each TX node senses its surrounding acoustic environment within its range R_T to create a list of available channels (LAC) [30]. The LAC is used by the TX and RX nodes such that they are informed about their individual available channels. In this process, the TX node sends a Request to Send (RTS) packet to the RX node over the CCC. The RTS includes the TX node's LAC list. If the RX node successfully receives the RTS packet and it has at least one free channel for communication, then the RX node replies instantly with a Clear to Send (CTS) over the CCC. The CTS packet is a short message including a clear to send flag for TX node and a backoff time for RX node's neighbors to avoid hidden terminal problem [5].

By receiving the RTS packet at the RX, the RX compares it with the channel states in its LAC. These channel states are represented by a $1 \times M$ vector that consists of binary elements indicating availability. Then, the receiver identifies the common elements of the received RTS channel vector and the corresponding elements of its own LAC channel vector. This results in a List of Confirmed Channels for Transmission (LCCT) which is created at the RX node [31].

The LCCT is also a $1 \times M$ vector in which each element is a binary value representing the available common data channels between the TX and RX nodes. The LCCT is sent by the RX to the TX node. When the TX node receives the LCCT packet from the RX node, it broadcasts this packet to its neighbors on the local CCC to inform them about the data channels that this TX-RX pair wishes to use. After computing and sharing the LCCT information for all TX-RX pairs, the nodes must use the LCCTs to compete for data channels.

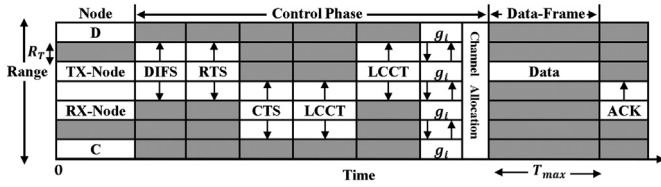


Fig. 4. Representation of the packet exchange between neighbor nodes. The RX node and Node D are in the transmission range of the TX node while the TX node and Node C are in transmission range of the RX node.

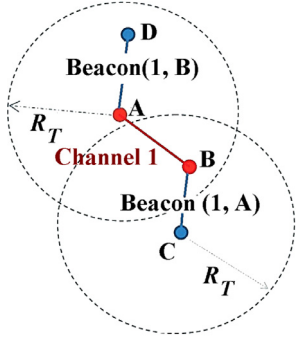


Fig. 5. The busy tone beacon ensures that Nodes D and C do not send RTS packets to Node A and B while they are communicating on Channel 1.

For a TX–RX pair i , a matrix L_i is computed where the j th row of the L_i matrix is the LCCT of the j th TX–RX neighboring pair to the i th pair. Thus L_i is a matrix of size $N_i \times M$ where N_i is the number of TX–RX pairs in the neighborhood of pair i .

The proposed MAC layer protocol does not require global synchronization among the ANs, and the contention access mechanism over the local CCC between the neighbors is based on the aforementioned BEB protocol for the JANUS Underwater Communications Standard [32].

The packet exchange in the initial phase of a channel allocation process is depicted in Fig. 4. The MAC protocol proposed employs three control packets : RTS, CTS, LCCT, as well as and the busy tone beacon. The duration of the data frame is T_{max} , its optimal size, depends on the load of the nodes and is heavily influenced by the bit error rate [12].

The purpose for the RTS/CTS packets includes (i) reserving the CCC and (ii) solving the hidden terminal problem by making the neighbor nodes aware of an upcoming transmission. Then, the LCCT handshake serves to synchronize the vacant channel information between each TX–RX pair and to prevent collisions between the ANs. Also, it ensures that the TX and RX nodes use the same set of vacant channels for data communication. After the initial negotiation phase is completed, the TX–RX pairs exchange a cost value g_i computed by the proposed algorithm, to assign the available channels to the TX–RX pairs with the lowest cost value. This will be detailed in Section 4. After assigning the data channel, the transmitter starts sending data over the data channel. While the TX and RX nodes transducers are busy sending and receiving on the data channel, their busy tone beacon generator broadcasts a periodic pulse to inform their neighbors that they are busy on the data channel; this prevents the multichannel hidden terminal problem. Fig. 5 illustrates the busy tone beacon generated by nodes A and B while communicating on Data Channel 1.

The channel access time during the control phase consists of a negotiation phase and a channel allocation which occurs on CCC. The overall end-to-end latency will be the time between the packet generation and the time of its correct delivery at the destination which includes the channel access time and propagation delay.

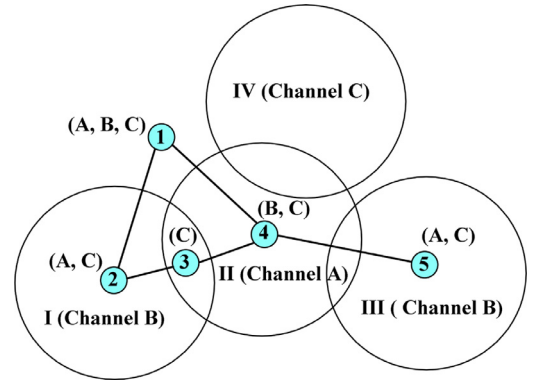


Fig. 6. Illustration of a neighboring pair's interference using the interference graph.

3.4. Graph model of the network

In this work the proposed algorithm utilizes the knowledge of the topology and channel sensing to minimize interference among TX–RX pairs during channel allocation. The local relationship between neighbor pairs and their available channels can be simplified into a graph model in which the vertices are TX–RX pairs and the edges represent interference among them. A set of available channels is assigned to each vertex which corresponds to its LCCT. Clearly, if two vertices are connected by an edge, they cannot both access the same channel simultaneously.

Fig. 6 illustrates a network in which there are five vertices to represent five TX–RX pairs. There are three channels: A, B and C which are opportunistically available for the AN pairs. Due to the sharing agreements, channels that are unavailable, e.g. shadow zones [33], cannot be utilized by ANs within their interference range (labeled I, II, III and IV). Each pair may access a different set of available channels. As shown in Fig. 6, channels A, B, and C are available for pair 1; channels A and C are available for pair 2, and so on for the rest of the pairs. Note that Fig. 6 depicts the network status at a fixed time instant.

The model proposed identifies the interference in the network, such that channels cannot be occupied by two neighbor nodes simultaneously. An undirected graph G is used, and represented by $G = (V, E, L)$, where $V = \{v_1, v_1, \dots, v_N\}$ is the set of vertices representing the TX–RX pairs, E is the set of edges representing interference among neighbor pairs and L is the set of available channels. We use an $N \times N$ matrix E to formulate the edge status, where N is the number of TX–RX pairs. At index (i, j) the edge status e_{ij} between two TX–RX pairs i and j is assigned 1 when vertices i and j are neighbors, otherwise it is equal to 0. Based on this definition, G is an undirected graph and effectively the interference matrix will be symmetric. The set of available channels for various pairs are stored in a global $N \times M$ matrix L , where at index (i, k) , $l_{ik} = 1$ if the channel k is available for the TX–RX pair i and $l_{ik} = 0$ indicates that it is not available. Recall that N is the number of TX–RX neighbor pairs and M is the number of channels. In other words, the i th row represents the LCCT of the i th TX–RX pair. Note that the local matrix L_i for the TX–RX pair i is a sub-matrix of L which contains only those rows of L that are corresponding to pair i neighbors.

We denote the set of assigned channels in the entire network by an $N \times M$ matrix S , where at index (i, k) , $s_{ik} = 1$ if the channel k is allocated to the pair i , otherwise, $s_{ik} = 0$. The i th row of the matrix S represents the channels which are allocated to i th pair by the channel allocation algorithm.

The performance metrics of the allocation algorithm can be measured and formulated in terms of S and L . Similarly to a technique developed in [4], the goal is to maximize the network spec-

Table 2
Parameters for the HCHF Algorithm.

R_T	Acoustic nodes transmission range
LAC	$1 \times M$ vector, List of available channels
RTS	Request to send packet
CTS	Clear To Send packet
DIFS	The time duration for which a TX node senses CCC
N_i	Number of TX–RX pairs in the neighborhood of pair i
LCCT _{i}	$1 \times M$ vector, List of confirmed channels for transmission in which the available common channels between TX and RX nodes are shown by 1 and the rest of channels by 0
\mathbf{L}_i	$N_i \times M$ matrix, rows of matrix \mathbf{L}_i is composed of the channels which are available for TX–RX pair i neighbors, e.g. j th row of matrix \mathbf{L}_i is the LCCT _{j} of TX–RX pair j th which is in the neighborhood of pair i
T_{\max}	Maximum packet duration
C_d	Chip duration
\mathbf{S}	$N \times M$ matrix of the entire network channels allocation
γ_i	Number of the channels obtained by pair i
σ^2	Variance of allocated channels to TX–RX pairs
\mathbf{IM}_i	$N_i \times M$ interference matrix for pair i
p_i	$1 \times M$ vector of non-contention channels of pair i . It is the set of available channels in the LCCT that cannot be used by neighbors
q_i	$1 \times M$ vector of available channels in LCCT that require contention with the neighbors to be acquired by pair i
$x_i(k)$	Number of neighbors for TX–RX pair i on channel k
g_i	the cost value of pair i to own at least one channel
μ_i	Channel possession threshold, $1 \leq \mu_i \leq \text{sum}(\text{LCCT}_i)$, constrains minimum and maximum channels acquisition

trum utilization S_U defined as

$$\max(S_U) = \max\left(\sum_{i=1}^N \sum_{k=1}^M s_{ik}\right) \quad (2)$$

subject to

$$s_{ik} \leq l_{ik}, s_{ik} \in 0, 1 \text{ and } s_{ik}s_{jk}e_{ij} = 0.$$

Note that N is the total number of TX–RX pairs and M is the number of channels. Then, for all pairs $i = \{1, \dots, N\}$ and channels $k = \{1, \dots, M\}$. Accordingly the optimization variable in the spectrum utilization problem is the number of utilized channels or summation of s_{ik} . The algorithm is also subject to the following fairness and coverage conditions:

1. The channel allocation between all the network pairs should have minimum variance σ^2 , where $\sigma^2 = \text{var}(\gamma)$ and channel allocation in the entire network is $\gamma_{1 \times N} = [\gamma_1, \gamma_2, \dots, \gamma_N]$ where γ_i is number of channels allocated to pair i , i.e.

$$\gamma_i = \sum_{k=1}^M s_{ik}. \quad (3)$$

2. The coverage constraints for pair i are such that $1 \leq \gamma_i$ for all $i = 1 \dots N$. This guarantees that each pair obtains at least one channel.

In the next section an allocation algorithm which can satisfy the above constraints is proposed. For this purpose, the fairness, the coverage, the channel assignment overhead and network utilization ratio are used as figure of merits.

4. High coverage and high fairness allocation

In this section, a distributed algorithm that attempts to maximize the network throughput is proposed. The algorithm also ensures allocation of a minimum of one data channel for each TX–RX pairs. The HCHF parameters and variables are summarized in Table 2.

The HCHF algorithm is described in six steps as follows:

1. First, each TX–RX pair i acquires its List of Confirmed Channels for Transmission (LCCT) and stores it in its LCCT _{i} vector. To ease the computations, the $N_i \times M$ interference matrix \mathbf{IM}_i is defined and is calculated by applying a logical AND operation between the pair i 's LCCT _{i} vector and every $j \in N_i$ neighbor's LCCT _{j} vector. The set of available channels in the LCCT _{i}

that cannot be used by neighbors are called the set of non-contention channels p_i . These channels can be easily identified by considering the zero columns of \mathbf{IM}_i and the corresponding nonzero elements of LCCT _{i} . Specifically, for each channel of $k \in M$, $p_i(k)$ is set to 1 if the k th column of \mathbf{IM}_i is zero and the k th column of LCCT _{i} is equal to 1.

The $1 \times M$ vector p_i initially represents the set of available channels that can be used by the TX–RX pair of i without needing any contention with its neighbors. During the allocation process, as a new channel is assigned to the TX–RX pair i , its corresponding element in p_i is set to 1. As such, at any time, the sum of elements of p_i , γ_i , represents the number of assigned channels to the TX–RX pair i , and as such $\gamma_i = \text{sum}(p_i)$.

Also, for each TX–RX pair i , a $1 \times M$ vector q_i is defined. The vector q_i represents the available channels in the TX–RX pair's LCCT _{i} that are common between neighbors. In other words, these are channels that are contentious for assignment between the neighbors. This vector is obtained by comparing the nonzero elements of LCCT _{i} with the nonzero columns of \mathbf{IM}_i . Effectively,

$$\text{LCCT}_i - p_i = q_i \quad (4)$$

The minimum required and maximum allowable number of channels for each TX–RX pair i is set by a threshold μ_i , where $1 \leq \mu_i \leq \text{sum}(\text{LCCT}_i)$, and is initialized with $\mu_i = 1$. As such, acquiring at least one data channel is attempted for each TX–RX pair. The threshold μ_i is increased by one if for all $j \in N_i$ neighbors of pair i , $\mu_i < \gamma_j$ or if neighbors of pair i do not have any available channels in their q_j to assign. The TX–RX pair i initiates a negotiation with its neighbors for the channel assignment until there is no channel available in q_i or the threshold μ_i reaches its maximum equal to $\text{sum}(\text{LCCT}_i)$. It should be noted that negotiation is only required between neighbors who have interference on certain channels. Furthermore, avoiding network congestion should be considered during the deployment such that the number of neighbors should always be less than the available channels $N_i < M$.

2. Considering that all packet exchanges occur only among neighbors, the following procedure continues until no available channel can be found to assign for the i th TX–RX pair's q_i vector: For each TX–RX pair i with $x_i(k)$ neighbors on a particular channel with $k \in (1, \dots, M)$, the probability that it is assigned the channel k will be $1/(x_i(k) + 1)$. The parameter $x_i(k)$ can be obtained as the sum of the elements of the k th column of \mathbf{IM}_i . For

each pair i , this probability is calculated to obtain at least one channel. Then $g_i(k)$, which is defined as the cost value for pair i to obtain channel k , is expressed as

$$g_i(k) = 1 - \prod_{\substack{k=1 \\ x_i(k)>0}}^{k=M} \left(1 - \frac{1}{x_i(k) + 1}\right) \quad (5)$$

As demonstrated in (5), it is assumed that the probability of obtaining a given channel is independent of the probability of obtaining other channels.

3. Next, for the j th neighbor of pair i , if the total number of possessed contention free channels are less than the threshold of μ_i (i.e. the sum of the p_i elements is smaller than μ_i) and channel k is available to assign their q_j vector, then all neighbor pairs exchange their g_j values and continue to step 4 otherwise if the sum of the p_i elements is greater or equal to μ_i the pair j give up the petition.
4. After receiving the g_j values from all the neighboring pairs $j \in N_i$, each TX-RX pair i decides if it has the minimum value among the g_j of its neighbors. If so, it selects the available channel with the lowest number, which is identified as the channel k in its contention channel list. It also announces itself and its selected channel to the neighbors by broadcasting a *ChannelAllocation* message over the local CCC containing a vector of assigned channels to TX-RX pair i . If two or more pairs have the same values of g_j , the deadlock can be broken by assigning the channel to the pair with the smaller ID. Note that the lowest channel index or node ID is used as a criterion for selection in the algorithm.
5. If the channel k is taken by the pair i , then it sets $p_i(k) = 1$. To avoid reallocation of the channel k to the pair i , this channel is removed from the list of available channels with a contention with pair i , i.e., $q_i(k) = 0$. Then, the neighboring pairs that interfere with pair i on channel k remove the allocated channel k from their list of available channels with contention. Specifically, $p_j(k)$ is cleared to 0 for all neighbors of the TX-RX pair i .
6. All neighbor pairs update their interference matrices of \mathbf{IM}_i and contention matrices of q_i . Then, until the sum of their assigned channels in p_i reaches the threshold μ_i , the algorithm iterates between steps 2–5. If all pairs reach the threshold of μ_i and there are still some channels in the contention matrix of some pairs, then the threshold variable of μ_i increments by 1 and steps 2–5 are repeated. Otherwise the algorithm ends. Consequently, when the contention matrices of all pairs become empty the allocation algorithm is terminated.

The allocation algorithm is summarized in Algorithm 1. Next, in Section 5, the algorithm is applied to a realistic underwater deployment.

5. Simulation results

In this section the performance of the proposed HCHF distributed channel allocation scheme is compared with conventional channel allocation techniques in the UWASN framework.

Fig. 7 illustrates the two-dimensional topology of a distributed network. In this simulation, a maximum of 144 ANs are randomly distributed in a dense area of 2.5×2.5 km to represent a future IoUT application. The total number of available channels are $M = 10$. Each channel occupies an equal bandwidth of 2-kHz between 10.5 kHz and 30.5 kHz. The authors in [34] observe that the probability of establishing an acoustic link in which the SNR is less or equal to a threshold δ is affected by various ambient factors, e.g. shadow zones. In this network model, it is assumed that channels may intermittently be in shadow zones. Here the ratio of number

Algorithm 1: HCHF algorithms.

```

1: Initialization: Define the LAC  $\forall$  node  $\in K$  ;
   Define  $LCCT_i \forall$  TX-RX  $\in N$  ;
for  $i = 1$  to  $N_i$  do
  |  $\mathbf{L}_i(i, :) = LCCT_i$ ;
end
for  $i = 1$  to  $N_i$  do
  | for  $j = 1$  to  $N_j$  do
  | |  $\mathbf{IM}_i(j, :) = LCCT_i \text{ AND } \mathbf{L}_i(j, :)$ 
  | end
end
for  $i = 1$  to  $N_i$  do
  | for  $j = 1$  to  $M$  do
  | | if  $\mathbf{IM}_i(:, j) = 0 \text{ AND } LCCT_i(j) = 1$  then
  | | |  $p_i(j) = 1$ 
  | | end
  | | if  $\mathbf{IM}_i(:, j) \neq 0 \text{ AND } LCCT_i(j) = 1$  then
  | | |  $q_i(j) = 1$ 
  | | end
  | end
end
2: while  $q_i = 0 \text{ OR } LCCT_i(:, :) = 0$  do
  | for  $i = 1$  to  $N_i$  do
  | | for  $k = 1$  to  $M$  do
  | | |  $x_i(k) = \text{sum} [\mathbf{IM}_i(:, k)]$ 
  | | end
  | |  $g_i(k) = 1 - \prod_{\substack{k=1 \\ x_i(k)>0}}^{k=M} \left(1 - \frac{1}{x_i(k)+1}\right)$ 
  | | end
  | end
  | 3: Exchange  $g_i$  AND  $\mu_i$ : for  $k = 1$  to  $M$  do
  | | if  $\text{sum} (p_i) < \mu_j$  and  $q_i(k) = 1$  and  $g_i < \min(g_j)$  then
  | | |  $p_i(k) = 1, q_i(k) = 0, \forall j \in N_i$  then  $q_j(k) = 0$ 
  | | end
  | | if  $\text{sum} (p_i) < \mu_j$  and  $q_i(k) = 1$ 
  | | and  $g_i = \min(g_j)$  and  $i < j$  then
  | | |  $p_i(k) = 1, q_i(k) = 0, \forall j \in N_i$  then  $q_j(k) = 0$ 
  | | end
  | end
  | 5: update interference and contention matrices: if
  |  $\forall j \in N_i, \forall k \in M \text{ sum}(p_j) = \mu_i$  and  $\text{sum}(q_j(k)) \neq 0$  then
  | |  $\mu_i = \mu_i + 1$  and continue from step 2 ;
  | else
  | | exit;
  | end

```

of reliable channels over the total number of channels is assumed to be $\lambda = 0.9$ in different hexagonal areas.

To manage the up-link communication to the surface and effectively reduce the nodes' manufacturing cost and battery supply, UWGs with cellular coverage are demonstrated in Fig. 7. Initially, UWGs are primary users and have priority to acquire the most reliable channel with highest SNR among $M = 10$ channels. The UWGs' selected channel is dedicated to communications between ANs and UWGs so it can not be assigned to peer-to-peer communications between ANs. As such, its access scheme is the same as for the CCC. The rest of the 8 available channels can be apportioned among ANs collaboratively.

To represent the propagation conditions, the maximum transmission range of the ANs is approximated to be 500 m. The proposed algorithm performance is compared with other algorithms by gradually increasing the number of participating ANs from 10 to 144 nodes. In each setting, the allocation algorithm runs one

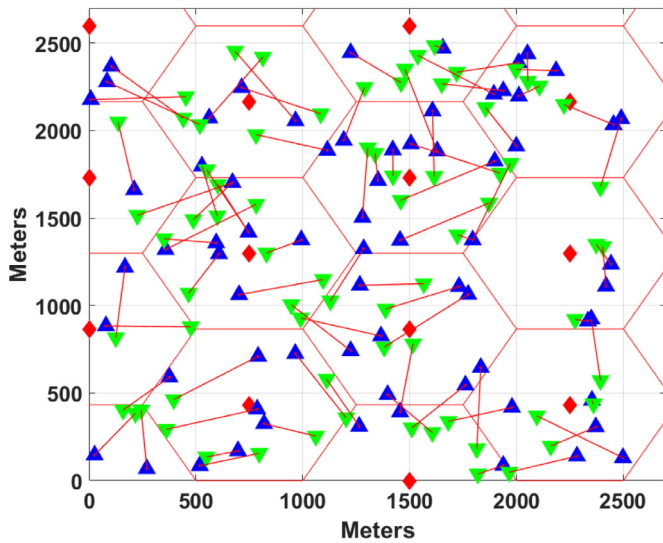


Fig. 7. Two-dimensional illustration of a network consisting of 72 TX-RX pairs. Green triangles are TX nodes and blue triangles are RX nodes, lines between TX-RX pairs show the corresponding communication links. Red diamonds are UWGs. (For interpretation of the references to colour in this figure legend, the reader is referred to the web version of this article.)

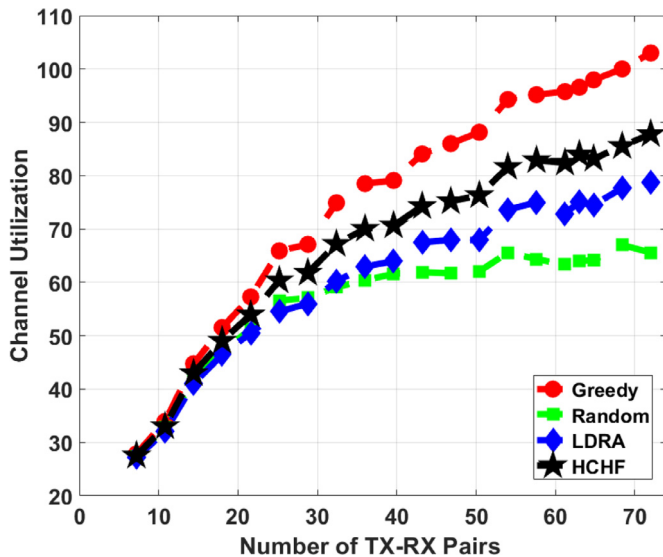


Fig. 8. Channel utilization of the TX-RX pairs defined as the total number of channels allocated to TX-RX pairs.

hundred times for randomly scattered nodes, and for each, a new observation of available channels is defined between the ANs. The performance of the algorithms is averaged over one hundred iterations to nullify the impact of the nodes' random scattering on the output of the algorithm.

The Greedy, Random and LDRA algorithms (described in Section 2) are compared with the HCHF algorithm in terms of channel utilization, fairness, network coverage among ANs and allocation process overhead which is measured by averaging the number of controlling packets that are exchanged by each TX-RX pair of ANs during the allocation process.

Fig. 8 represents the channel utilization, defined as the total number of channels assigned to the TX-RX pairs in the entire network. As expected, the Greedy algorithm approach can allocate the maximum number of available channels among these algorithms. The Greedy method, in which the channels are allocated to pairs with better conditions, provides the best network utilization.

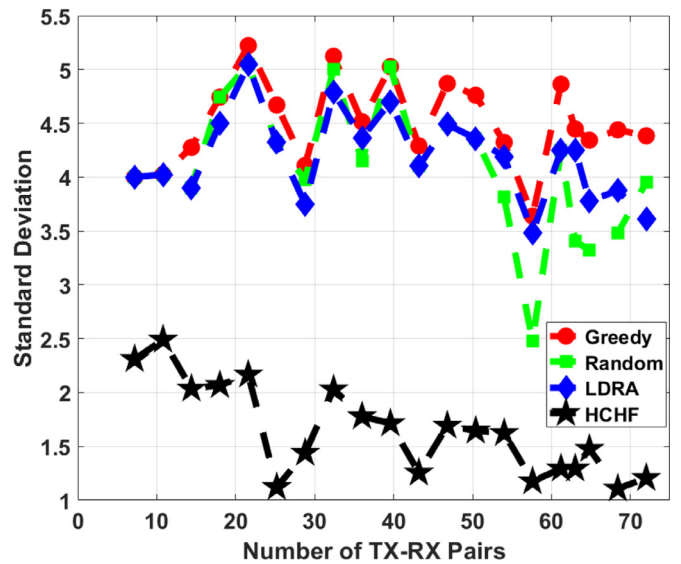


Fig. 9. Evaluation of the standard deviation of allocated channels.

Note that all algorithms perform very differently when the channel demand is increasing. However, in lower AN traffic, they have very similar performance, because there is less contention among the ANs. Note that the R_T can directly affect interference among ANs. Decreasing the R_T decreases the interference. Therefore, it increases the possibility of more allocations and provides a better utilization for all algorithms. However, for a small acoustic range, it will result in network disconnectivity among ANs which is not desired. The simulation results indicate that the HCHF algorithm has a better utilization performance in comparison to the random algorithm and LDRA. The reason is that HCHF attempts to manage fairness without sacrificing the network utilization.

Next, the standard deviation of allocated channels to the TX-RX pairs is used as a metric for comparing the fairness of the allocation algorithms. A large standard deviation means that there is a significant gap between the numbers of channels allocated among different pairs. Fig. 9 shows that the standard-deviation parameter of HCHF is lower than that of other allocation algorithms. The Greedy algorithm has the highest standard-deviation, and as such, it is very unfair. By increasing the number of TX-RX pairs, the variance of allocations in the HCHF algorithm is converging to its minimum, though from Fig. 8 it can be seen that HCHF algorithm channel utilization is high.

The number of TX-RX pairs that have received at least one channel, where the channel possession threshold is $\mu = 1$, is another metric that is used to evaluate coverage. This parameter is also an indication of the network connectivity in multihop relaying scenarios. Fig. 10 shows the number of TX-RX pairs which have received a minimum of one channel out of all the TX-RX pairs in the network. As can be observed, HCHF can cover the maximum number of ANs.

The control packets overhead is defined as the average number of signalling packets transmitted by each TX-RX Pairs to its neighbors during the control phase. In Fig. 11, the average number of exchanged packets per each TX-RX pair is shown for different algorithms. As the network density increases, the number of neighbor nodes on all the channels increases which imposes more interference on the network. Consequently, to solve the channel assignment problem and avoid collision more controlling packets are needed. It is important to find an optimum network density to avoid excessive congestion and keep the number of controlling packets as low as possible because more controlling packets results

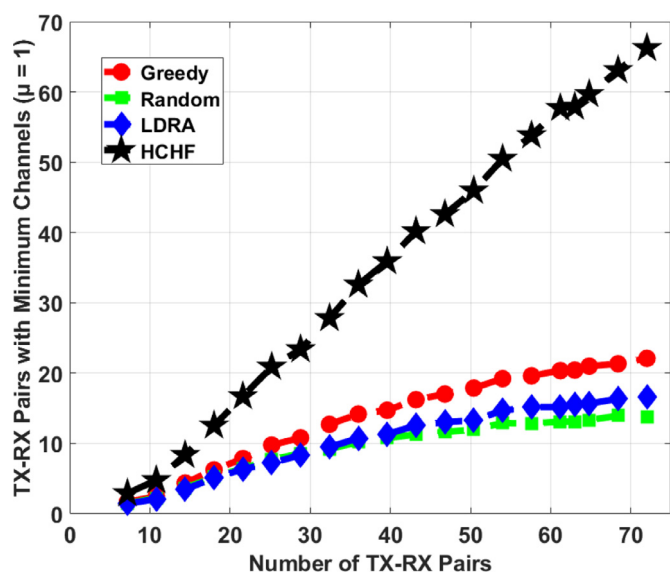


Fig. 10. Evaluation of the network coverage.

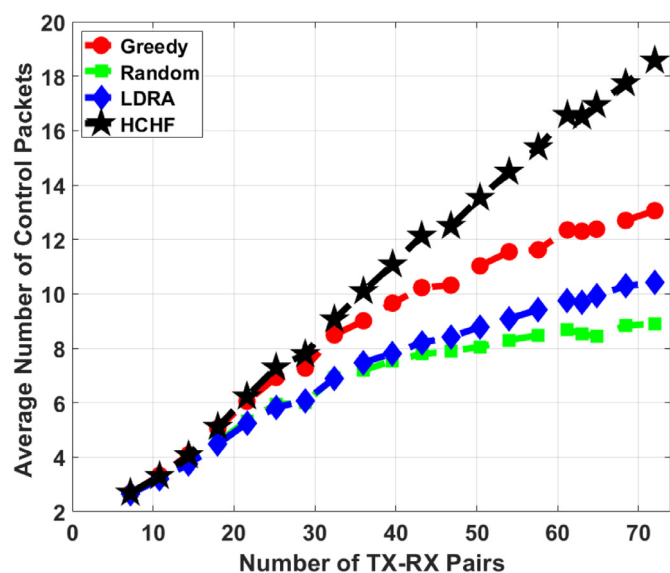


Fig. 11. Evaluation of average number of control packets submitted by each TX-RX pair during the control phase.

in more energy consumption and extreme delay. From Fig. 11 it can be seen that the control packets overhead distance between HCHF and the other algorithms overshoots when the number of TX-RX pairs in the network exceeds more than 50 TX-RX pairs. In this set-up, a maximum density of 100 ANs per 2.5×2.5 km or 16 ANs per km² can be considered as the optimum network density where the HCHF performs efficiently.

6. Conclusion

In this paper, a new distributed channel allocation algorithm for UWASNs called HCHF has been described. HCHF employs a graph for modelling interference constraints among the ANs. The algorithm ensures that the ANs within the transmitting range of each other do not utilize the same frequency channels. HCHF allocates the channels to ANs in a way that allows at least one channel to be assigned to each TX-RX pair. To optimize fairness, HCHF tries to balance the number of allocated channels to the ANs and increases the network coverage. Moreover, the performance has been

compared to that of three existing distributed channel allocation algorithms: the Greedy, Random and LDRA algorithms. To evaluate and compare the HCHF algorithm with these channel allocation algorithms, several computer simulations have been carried out. The simulations indicate that HCHF surpasses other algorithms in terms of fairness since it tries to allocate at least one channel to each node. The greedy algorithm tends to maximize the channel utilization by sacrificing fairness. The random algorithm has a low throughput, and LDRA offers lower throughput and fairness. It is shown that the improved channel utilization and fairness provided by HCHF is constrained on the overhead of the control packets.

Finally, for a reliable and efficient channel assignment in UWASN, an optimum network density should be taken into account to avoid excessive overhead, energy consumption and access delay on the CCC.

Conflict of interest

We wish to confirm that there are no known conflicts of interest associated with this publication and there has been no significant financial support for this work that could have influenced its outcome.

Supplementary material

Supplementary material associated with this article can be found, in the online version, at doi:10.1016/j.comnet.2019.05.011.

References

- [1] E. Liou, C. Kao, C. Chang, Y. Lin, C. Huang, Internet of underwater things: challenges and routing protocols, in: 2018 IEEE International Conference on Applied System Invention (ICASI), 2018, pp. 1171–1174.
- [2] E.M. Sozer, M. Stojanovic, J.G. Proakis, Underwater acoustic networks, *IEEE J. Ocean. Eng.* 25 (1) (2000) 72–83.
- [3] J.A. Catipovic, Performance limitations in underwater acoustic telemetry, *IEEE J. Ocean. Eng.* 15 (3) (1990) 205–216.
- [4] W. Wang, X. Liu, List-coloring based channel allocation for open-spectrum wireless networks, in: IEEE 62nd Veh. Techn. Conf., 2005., 1, 2005, pp. 690–694.
- [5] Z. Zhou, Z. Peng, J.H. Cui, Z. Jiang, Handling triple hidden terminal problems for multichannel MAC in long-Delay underwater sensor networks, *IEEE Trans. Mob. Comput.* 11 (1) (2012) 139–154.
- [6] N. Baldo, P. Casari, M. Zorzi, Cognitive spectrum access for underwater acoustic communications, in: ICC Workshops - 2008 IEEE International Conference on Communications Workshops, 2008, pp. 518–523.
- [7] J. An, H. Kim, H. Lee, J. Chung, Low collision random access using grouping nodes in underwater communications, in: 2017 Ninth International Conference on Ubiquitous and Future Networks (ICUFN), 2017, pp. 767–769.
- [8] Y. Luo, L. Pu, H. Mo, Y. Zhu, Z. Peng, J.H. Cui, Receiver-Initiated spectrum management for underwater cognitive acoustic network, *IEEE Trans. Mob. Comput.* 16 (1) (2017) 198–212.
- [9] J. Wang, Y. Huang, H. Jiang, Improved algorithm of spectrum allocation based on graph coloring model in cognitive radio, in: 2009 WRI International Conference on Communications and Mobile Computing, 3, 2009, pp. 353–357.
- [10] G. Zhang, S. Feng, Subcarrier allocation algorithms based on graph-coloring in Cognitive Radio NC-OFDM system, in: 2010 3rd Intl. Conf. Computer Science and Information Technology, 2, 2010, pp. 535–540.
- [11] I.F. Akyildiz, D. Pompili, T. Melodia, Underwater acoustic sensor networks: research challenges, *Ad Hoc Netw.* 3 (3) (2005) 257–279.
- [12] S. Basagni, C. Petrioli, R. Petrocchia, M. Stojanovic, Choosing the packet size in multi-hop underwater networks, in: OCEANS'10 IEEE SYDNEY, 2010, pp. 1–9.
- [13] A.A. Syed, W. Ye, J. Heidemann, T-Lohi: a new class of MAC protocols for underwater acoustic sensor networks, in: IEEE INFOCOM 2008 - The 27th Conference on Computer Communications, 2008, pp. 789–797.
- [14] A.A. Syed, J. Heidemann, W. Ye, Tones for real: managing multipath in underwater acoustic wakeup, in: 2010 7th Annual IEEE Communications Society Conference on Sensor, Mesh and Ad Hoc Communications and Networks (SECON), 2010, pp. 1–3.
- [15] S.-L. Wu, C.-Y. Lin, Y.-C. Tseng, J.-L. Sheu, A new multi-channel mac protocol with on-demand channel assignment for multi-hop mobile ad hoc networks, in: Proceedings International Symposium on Parallel Architectures, Algorithms and Networks, I-SPAN 2000, 2000, pp. 232–237.
- [16] T. Chen, H. Zhang, G.M. Maggio, I. Chlamtac, Cogmesh: a cluster-based cognitive radio network, in: 2007 2nd IEEE International Symposium on New Frontiers in Dynamic Spectrum Access Networks, 2007, pp. 168–178.

- [17] P. Qarabaqi, M. Stojanovic, Statistical characterization and computationally efficient modeling of a class of underwater acoustic communication channels, *IEEE J. Ocean. Eng.* 38 (4) (2013) 701–717.
- [18] M. Chitre, A high-frequency warm shallow water acoustic communications channel model and measurements, *J. Acoust. Soc. Am.* 122 (5) (2007) 2580–2586.
- [19] W.-B. Yang, T.C. Yang, High-frequency channel characterization for M-ary frequency-shift-keying underwater acoustic communications, *J. Acoust. Soc. Am.* 120 (5) (2006) 2615–2626.
- [20] X. Cheng, L. Yang, X. Cheng, Cognitive spectrum access for underwater acoustic communications, in: *Cooperative OFDM Underwater Acoustic Communications*, Springer International Publishing, 2016, pp. 13–16.
- [21] Y. Zhou, A. Song, F. Tong, Underwater acoustic channel characteristics and communication performance at 85 kHz, *J. Acoust. Soc. Am.* 142 (4) (2017) EL350–EL355.
- [22] M. Stojanovic, J. Preisig, Underwater acoustic communication channels: propagation models and statistical characterization, *IEEE Commun. Mag.* 47 (1) (2009) 84–89.
- [23] P.A. van Walree, F. Socheleau, R. Otnes, T. Jenserud, The watermark benchmark for underwater acoustic modulation schemes, *IEEE J. Ocean. Eng.* 42 (4) (2017) 1007–1018.
- [24] B. Li, S. Zhou, M. Stojanovic, L. Freitag, P. Willett, Multicarrier communication over underwater acoustic channels with nonuniform doppler shifts, *IEEE J. Ocean. Eng.* 33 (2) (2008) 198–209.
- [25] J. Potter, J. Alves, D. Green, G. Zappa, I. Nissen, K. McCoy, The JANUS underwater communications standard, in: *2014 Underwater Communications and Networking (UComms)*, 2014, pp. 1–4.
- [26] J. Alves, et al., Moving JANUS forward: a look into the future of underwater communications interoperability, in: *OCEANS 2016 MTS/IEEE Monterey*, 2016, pp. 1–6.
- [27] A. Viterbi, Convolutional codes and their performance in communication systems, *IEEE Trans. Commun. Technol.* 19 (5) (1971) 751–772.
- [28] D. Green, Establishing a standard for underwater digital acoustic communications and networks, in: *Proceedings of the 10th International Conference on Underwater Networks & Systems*, in: *WUWNET '15*, ACM, New York, NY, USA, 2015, pp. 20:1–20:5.
- [29] M. Stojanovic, J.G. Proakis, J.A. Rice, M.D. Green, Spread spectrum underwater acoustic telemetry, in: *IEEE Oceanic Engineering Society. OCEANS'98. Conference Proceedings*, 2, 1998, pp. 650–654 vol.2.
- [30] C. Cordeiro, K. Challapali, C-MAC: a cognitive MAC protocol for multi-channel wireless networks, in: *2007 2nd IEEE Intl. Symp. New Frontiers in Dynamic Spectrum Access Networks*, 2007, pp. 147–157.
- [31] L. Cao, H. Zheng, Distributed rule-regulated spectrum sharing, *IEEE J. Sel. Areas Commun.* 26 (1) (2008) 130–145.
- [32] S. Jiang, State-of-the-Art medium access control (MAC) protocols for underwater acoustic networks: A Survey based on a MAC reference model, *IEEE Commun. Surv. Tutor.* 20 (1) (2018) 96–131.
- [33] M.C. Domingo, A topology reorganization scheme for reliable communication in underwater wireless sensor networks affected by shadow zones, *Sensors* 9 (11) (2009) 8684–8708.
- [34] Q. Wang, H.-N. Dai, C.F. Cheang, H. Wang, Link connectivity and coverage of underwater cognitive acoustic networks under spectrum constraint, *Sensors* 17 (12) (2017).



Hossein is currently Ph.D. student in electrical engineering program at Dalhousie university. He received his Master's degree in communication systems from Shiraz university, Iran. In his Master he worked on dynamic spectrum allocation and maximizing throughput in cognitive ad hoc networks. His interest in underwater sensor networks led him to join UWSTREAM lab, under the supervision of Dr. Jean-Francois Bousquet. His research is now focusing on underwater wireless sensor networks to enable ocean monitoring and communication infrastructure for industrial applications such as offshore oil and gas exploration and pipelines surveillance.



Jean-François Bousquet joined Dalhousie University in July 2013 and is currently Associate Professor in the Department of Electrical and Computer Engineering. His research interests are communication systems, highly integrated circuits, and software defined radios applied to ocean technology. He is a graduate of École Polytechnique de Montréal where he completed his B.Eng. in Electrical Engineering in 2001. He also completed his M.Sc. and Ph.D. degree in Electrical Engineering at the University of Calgary in 2007 and 2011 respectively, where he focused on the implementation of low-power integrated circuits applied to wireless communications. Between 2009 and 2011, he was employed as a high-speed analog IC designer at Ciena for the development of coherent fibre optics communication networks. Since he joined Dalhousie, he has applied his expertise towards a new and exciting application: underwater communications.